Inorganic Chemistry

ARTICLE

pubs.acs.org/IC

$[(Ph)_3PBr][Br_7]$, $[(Bz)(Ph)_3P]_2[Br_8]$, $[(n\text{-}Bu)_3MeN]_2[Br_{20}]$, $[C_4MPyr]_2[Br_{20}]$, and $[(Ph)_3PCl]_2[Cl_2I_{14}]$: Extending the Horizon of Polyhalides via Synthesis in Ionic Liquids

Michael Wolff, Alexander Okrut, and Claus Feldmann*

Institut für Anorganische Chemie, Karlsruhe Institute of Technology (KIT), Engesserstrasse 15, D-76131 Karlsruhe, Germany

Supporting Information

ABSTRACT: The five polyhalides $[(Ph)_3PBr][Br_7]$, $[(Bz)(Ph)_3P]_2[Br_8]$, $[(n\text{-}Bu)_3MeN]_2[Br_{20}]$, $[C_4MPyr]_2[Br_{20}]$ ($[C_4MPyr]$ = *N*-butyl-*N*-methylpyrrolidinium), and $[(Ph)_3PCl]_2[Cl_2I_{14}]$ were prepared by the reaction of dibromine and iodine monochloride in ionic liquids. The compounds $[(Ph)_3PBr][Br_7]$ and $[(Bz)(Ph)_3P]_2[Br_8]$ contain discrete pyramidal $[Br_7]^-$ and Z-shaped $[Br_8]^{2-}$ polybromide anions. $[(n\text{-}Bu)_3MeN]_2[Br_{20}]$ and $[C_4MPyr]_2[Br_{20}]$ exhibit new infinite two- and three-dimensional polybromide networks and contain the highest percentage of dibromine ever observed in a compound. $[(Ph)_3PCl]_2[Cl_2I_{14}]$ also consists of a three-dimensional network and is the first example of an infinite polyiodine chloride. All compounds were obtained from ionic liquids as the solvent that, on the one hand, guarantees for a high stability against strongly oxidizing Br_2 and ICl and that, on the other hand, reduces the high volatility of the molecular halogens.

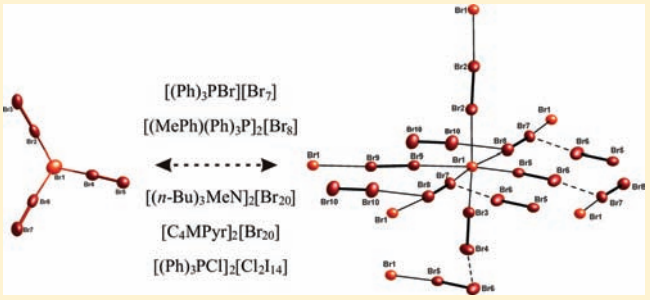

INTRODUCTION

The existence of polyhalides was first suggested by Jörgensen in 1871.[1] The salt $[NH_4][I_3]$ was identified as the first example and validated by crystal-structure determination later in 1935.[2] Since then, polyhalides have been the subject of intensive research efforts and have become standard chemistry textbook knowledge during the last 80 years.[3,4] The largest number of known compounds is related to polyiodides, which have considerable structural diversity.[5] Their composition can be rationalized based on the general composition $[I_{m+n}]^{n-}$ [with m ($I^{\pm 0}$) and n (I^{-I})], ranging from $[I_3]^-$ as the smallest representative, through discrete polyiodide species (e.g., $[I_{26}]^{3-}$ and $[I_{29}]^{3-}$) to infinite-chain- and layer-type networks.[5−8] Much less is known regarding the lighter and more reactive halogens. Thus, polybromides are limited to $[Br_3]^-$, linear $[Br_4]^{2-}$, Z-shaped $[Br_8]^{2-}$ and ring-type $[Br_{10}]^{2-}$.[9−11] Moreover, the two compounds $[C_5H_6S_4Br]^+[(Br_3^-)(^1/_2Br_2)]$ and $[H_4Tppz^{4+}][(Br^-)_2(Br_4^{2-})]$ [H_4Tppz = tetra(2-pyridyl)pyrazinium] contain infinite-chain-like polybromide anions.[12,13] The salt $[TtddBr_2]^{2+}[(Br^-)_2(Br_2)_3]$ ($[TtddBr_2]^{2+}$ = 4,5,9,10-tetrathiocino[1,2-*b*:5,6-*b*′]-1,3,6,8-tetraethyldiimidazolyl-2,7-dibromodithionium) represents the only example of an infinite two-dimensional (2D) polybromide network.[14] With regard to chlorine and fluorine derivatives, only $[Cl_3]^-$, V-shaped $[(Cl_3)(Cl_2)]^-$, and $[F_3]^-$ have been reliably identified so far.[15−17]

Despite their role in the basic chemistry of halogens, polyhalides are relevant for certain types of applications also. Here, the redox system $I^-/[I_3]^-$ of classical analytical chemistry is the most prominent.[18] Moreover, polyiodides play an essential role in extending the area of dye-sensitized thin-film solar cells (also called Grätzel cells).[19] Polyiodides and polybromides have also been discussed in the context of high-power batteries or antimicrobial filters and textiles.[20,21] In addition, polybromides have been evaluated as reactive species in Suzuki- or Heck-type coupling reactions[22,23] as well as in zinc−bromine batteries.[24] Thus, knowledge on the existence and stability of novel polyhalides can contribute to all of these areas and may initiate novel types of applications.

We now report on the novel compounds $[(Ph)_3PBr][Br_7]$, $[(Bz)(Ph)_3P]_2[Br_8]$, $[(n\text{-}Bu)_3MeN]_2[Br_{20}]$, and $[C_4MPyr]_2[Br_{20}]$ containing the discrete anions $[Br_7]^-$ and $[Br_8]^{2-}$ as well as infinite 2D and three-dimensional (3D) polybromide networks. $[(Ph)_3PCl]_2[Cl_2I_{14}]$, moreover, is obtained as the first example of a polyiodine chloride 3D network. In addition, $[(n\text{-}Bu)_3MeN]_2[Br_{20}]$ and $[C_4MPyr]_2[Br_{20}]$ with nine molecules of dibromine contain the highest percentage of elemental bromine ever observed in a compound. All of the above polyhalides were obtained via a comparably facile and straightforward strategy: synthesis in ionic liquids.

EXPERIMENTAL METHODS

General Procedures. All synthetic work and sample manipulation was performed using standard Schlenk techniques or gloveboxes. The synthesis of the ionic liquids $[C_{10}MPyr]Br$ and $[(n\text{-}Bu)_3MeN][N(Tf)_2]$

Received: August 2, 2011
Published: October 25, 2011

Table 1. Crystallographic Data of Polyhalides (T = 200 K; λ(Mo Kα) = 71.073 pm)

	$[(Ph)_3PBr][Br_7]$	$[(Bz)(Ph)_3P]_2[Br_8]$	$[(n\text{-}Bu)_3MeN]_2[Br_{20}]$	$[C_4MPyr]_2[Br_{20}]$	$[(Ph)_3PCl]_2[Cl_2I_{14}]$
fw/g mol^{-1}	901.55	673.04	999.48	941.36	1221.47
space group, Z	$P2_1$, 2	$P\bar{1}$, 2	$C2/c$, 8	$P\bar{1}$, 2	$P2_1/c$, 4
a/pm	1062.5(2)	904.5(2)	1634.0(3)	847.5(2)	1150.5(2)
b/pm	1209.1(3)	964.3(2)	1024.2(2)	1099.6(2)	1758.1(3)
c/pm	1073.2(2)	1434.8(3)	3315.4(7)	1313.8(3)	1767.0(6)
α/deg	90	103.77(3)	90	88.77(3)	90
β/deg	115.23(3)	93.72(3)	96.67(3) °	80.12(3)	123.02(2)
γ/deg	90	93.73(3)	90	75.85(2)	90
V/10^6 pm^3	1247.2(4)	1208.7(4)	5511.3(19)	1169.3(4)	2996.8(13)
ρ_{calc}/g cm^{-3}	2.401	1.849	2.409	2.674	2.707
μ/cm^{-1}	12.93	6.736	14.543	17.127	7.487
R1/wR2 [$I \geq 2\sigma(I)$]	0.056/0.128	0.037/0.094	0.050/0.109	0.043/0.097	0.039/0.098
R1/wR2 (all data)	0.072/0.142	0.051/0.100	0.084/0.121	0.081/0.111	0.049/0.102

was carried out as described elsewhere.[25,26] The ionic liquid $[C_4MPyr]OTf$ was purchased from IOLITEC. All additional starting materials, including Br_2 (99.9%) and ICl (99.9%), were obtained from ABCR.

All of the prepared polyhalides are extremely sensitive to moisture and contact with air. With regard to the low melting point of the compounds, suited single crystals for structure determination and refinement were selected at about −20 °C under a cooled nitrogen flow and mounted in perfluoropolyalkyl ether oil on top of a glass fiber. The purification of larger quantities of polyhalides was, however, not straightforward. Because the title compounds contain the same or a cation similar to that of the ionic liquid, the solubility of both is largely similar in typical organic solvents. For this reason, polyhalides are best separated from the ionic liquid on a glass frit under cooled nitrogen by washing three to four times with small portions of dried, ice-cooled acetonitrile or diethyl ether. Thereafter, the title compounds can be dried in a flow of cooled nitrogen. Although large quantities of all polyhalides are accessible in principle, complete separation of the ionic liquid via the above washing procedure due to concurrent partial dissolution of the polyhalides, nevertheless, reduces the final yield of the pure compounds significantly. In summary, the solubility as well as the temperature and moisture sensitivity of the polyhalides hampers the separation of large quantities of the title compounds as required for comprehensive analytical characterization. In the case of $[(n\text{-}Bu)_3MeN]_2[Br_{20}]$ and $[C_4MPyr]_2[Br_{20}]$, we were, however, successful in separating sufficient quantities of the pure compounds (i.e., 50−100 mg).

Thermogravimetry (TG) and differential thermoanalysis were performed with a STA409C device (Netzsch, Selb, Germany). The measurements were performed in dried nitrogen. Crystals of $[(n\text{-}Bu)_3MeN]_2[Br_{20}]$ and $[C_4MPyr]_2[Br_{20}]$ were selected under a flow of cool nitrogen (20 mg in corundum crucibles) and heated thereafter from room temperature to +600 °C at a rate of 10 °C min^{-1}. While $[(n\text{-}Bu)_3MeN]_2[Br_{20}]$ as well as $[C_4MPyr]_2[Br_{20}]$ melt at +5 to +10 °C, both compounds were in the liquid state when starting the TG analysis. Note, furthermore, that minor amounts of black carbon remained inside the crucible.

$[(Ph_3)PBr][Br_7]$. Dissolving triphenylphosphine (343 mg) in an eutectic, equimolar mixture of the ionic liquids $[C_{10}MPyr]Br$ (400 mg) and $[C_4MPyr][OTf]$ (380 mg) (with $[C_{10}MPyr]$ = *N*-decyl-*N*-methylpyrrolidinium; $[C_4MPyr]$ = *N*-butyl-*N*-methylpyrrolidinium; [OTf] = triflate) at +100 °C, followed by the addition of an excess of molecular dibromine (0.33 mL) at +50 °C, led to a light-red solution. Cooling this solution to room temperature resulted in the formation of large quantities of light-red, plate-shaped single crystals of $[(Ph)_3PBr][Br_7]$. Subsequent to washing and removal of the ionic liquid, the compound was obtained with a yield of about 40%.

$[(Bz)(Ph)_3P]_2[Br_8]$. Dissolving benzyl(triphenyl)phosphonium bromide (338 mg) in a eutectic, equimolar mixture of the ionic liquids $[C_{10}MPyr]Br$ (400 mg) and $[C_4MPyr][OTf]$ (380 mg) (with $[C_{10}MPyr]$ = *N*-decyl-*N*-methylpyrrolidinium; $[C_4MPyr]$ = *N*-butyl-*N*-methylpyrrolidinium; [OTf] = triflate) at +100 °C, followed by the addition of excess molecular dibromine (0.20 mL) at +50 °C, led to a light-red solution. Cooling to room temperature resulted in the formation of cubelike, light-red single crystals of $[(Bz)(Ph)_3P]_2[Br_8]$. Subsequent to washing and removal of the ionic liquid, the compound was obtained with a yield of about 20%.

$[(n\text{-}Bu)_3MeN]_2[Br_{20}]$. By the addition of an excess of molecular dibromine (0.13 mL) to a solution of (2-bromophenyl)diphenylphosphine (223 mg) in the ionic liquid $[(n\text{-}Bu)_3MeN][N(Tf)_2]$ (0.10 mL) [with $[(n\text{-}Bu)_3MeN]^+$ = (tributylmethyl)ammonium; $[N(Tf)_2]$ = bis(trifluoromethanesulfonyl)imide] and by subsequent heating to a temperature of +50 °C, a light-red solution was obtained. Cooling to −15 °C resulted in precipitation of the title compound as well as in partial crystallization of the ionic liquid. Large quantities of deep-red single crystals were obtained by slowly thawing this mixture to +5 °C. Note that the title compound was again completely dissolved at a temperature of +10 °C. Subsequent to washing and removal of the ionic liquid, the compound was obtained with a yield of about 50%.

$[C_4MPyr]_2[Br_{20}]$. By the addition of an excess of dibromine (0.33 mL) to a eutectic, equimolar mixture of the ionic liquids $[C_{10}MPyr]Br$ (400 mg) and $[C_4MPyr][OTf]$ (380 mg) (with $C_{10}MPyr$ = *N*-decyl-*N*-methylpyrrolidinium; C_4MPyr = *N*-butyl-*N*-methylpyrrolidinium; [OTf] = triflate), a light-red solution was obtained. Cooling from room temperature to −15 °C resulted in precipitation of the title compound as well as in partial crystallization of the ionic liquid. Deep-red, highly adhesive single crystals were obtained in large quantities by slowly thawing this mixture to +5 °C. Note that the title compound was again completely dissolved at a temperature of +10 °C. Subsequent to washing and removal of the ionic liquid, the compound was obtained with a yield of about 80%.

$[(Ph)_3PCl]_2[Cl_2I_{14}]$. By the addition of an excess of ICl (248 mg) to a solution of triphenylphosphane (100 mg) and the ionic liquid $[C_4MPyr][OTf]$ (0.10 mL) (with $[C_4MPyr]$ = *N*-butyl-*N*-methylpyrrolidinium; [OTf] = triflate), a dark-red solution was obtained. Cooling from room temperature to +6 °C resulted in crystallization of the title compound under the formation of a few deep-red, plate-shaped single crystals. Subsequent to washing and removal of the ionic liquid, the compound was obtained with a yield of about 10%.

X-ray Data Collection and Structure Solution. Data collection was performed at 200 K on an IPDS II image-plate diffractometer (Stoe, Darmstadt) using graphite-monochromatized Mo Kα (71.073 pm) radiation and a low-temperature device. After data reduction via *X-RED* (Stoe, Data Reduction Program, version 1.14, Darmstadt, 1999), space group determination was carried out on the basis of systematic

absences via *XPREP* (Stoe, Data Reduction Program, version 1.14, Darmstadt, 1999). Structure solution and refinement were performed by direct methods and refined by full-matrix least squares on F^2 with *SHELXTL* (Bruker, Structure Solution and Refinement Package, version 5.1, Karlsruhe, 1998). Non-H atoms were refined with anisotropic parameter of displacement. The position of the H atom could not be fixed via Fourier refinement and was therefore modeled based on idealized C−H bonds. *X-SHAPE* (Stoe, Crystal Optimisation for Numerical Absorption Correction, version 1.06, Darmstadt, 1999) was used to apply numerical absorption correction based on crystal-shape optimization. Illustrations of the crystal structures were prepared via *DIAMOND* (Crystal Impact, Visuelles Informationssystem für Kristallstrukturen, version 3.0d, Bonn, 2005). Details regarding crystal structure determination and refinement are summarized in Table 1 and are deposited in the Supporting Information.

RESULTS AND DISCUSSION

Ionic-Liquid-Based Synthesis of Polyhalides. In view of the synthesis of polyhalides $[(Ph)_3PBr][Br_7]$, $[(Bz)(Ph)_3P]_2[Br_8]$, $[(n\text{-}Bu)_3MeN]_2[Br_{20}]$, $[C_4MPyr]_2[Br_{20}]$, and $[(Ph)_3PCl]_2[Cl_2I_{14}]$, the ionic liquids $[C_4MPyr][OTf]$, $[C_{10}MPyr]Br$, and $[(n\text{-}Bu)_3MeN][N(Tf)_2]$ exhibit several beneficial features. First, the ionic liquids are stable toward strongly oxidizing starting materials such as elemental bromine and iodine monochloride. Second, the observed low vapor pressure of Br_2 and ICl in the applied ionic liquids is highly relevant. Qualitatively, this can be visualized by the absence of the characteristic deep-brown (Br_2) and brownish-red (ICl) color above the liquid phase at moderate temperatures (i.e., +10 to +30 °C). Finally, the combination of $[C_{10}MPyr]Br$ and $[C_4MPyr][OTf]$ turned out to be exceptionally advantageous.[27] Herein, $[C_{10}MPyr]Br$ serves as a "bromide donor", whereas $[C_4MPyr][OTf]$ acts as a "liquifier" to establish an eutectic mixture that is even liquid below room temperature and thereby allows growing suited single crystals of the low-melting halogen-rich compounds below room temperature (i.e., at −20 °C to +10).

The successful preparation of novel polyhalides also points to the role that ionic liquids may play regarding the synthesis of highly reactive compounds in the future.[28−30] To this concern, the reaction of elemental metals and chalcogens in ionic liquids has already led to interesting results. This includes, for instance, a fascinating chlathrate-type germanium modification (i.e., $\square_{24}Ge_{136}$),[31] the observation of sulfur as a noncharged ligand (e.g., $[(\eta^1\text{-}S_8)Cu(1,5,9\text{-}\eta^3\text{-}S_{12})][Al(OR^F)_4]$)[32] or promising layer-type thermoelectrical materials (e.g., $[Bi_2Te_2Br][AlCl_4]$).[33] In contrast, the chemistry of halogens in ionic liquids is dominated by halogenidometalates exhibiting discrete or network-like building units.[34−37] Reactions involving elemental halogens and polyhalides, in contrast, have been sparsely performed. Thus, the polyhalides $[(Ph)_3PBr][Br_7]$, $[(Bz)(Ph)_3P]_2[Br_8]$, $[(n\text{-}Bu)_3MeN]_2[Br_{20}]$, $[C_4MPyr]_2[Br_{20}]$, and $[(Ph)_3PCl]_2[Cl_2I_{14}]$ represent the first halogen-rich compounds prepared via an ionic-liquid-based approach.

$[(Ph)_3PBr][Br_7]$. $[(Ph)_3PBr][Br_7]$ was obtained as light-red, plate-shaped crystals from an equimolar mixture of the ionic liquids $[C_{10}MPyr]Br$ and $[C_4MPyr][OTf]$, containing dissolved $(Ph)_3P$ and molecular dibromine in excess. According to crystal structure analysis based on single crystals, the title compound crystallizes monoclinically and surprisingly exhibits the polar, noncentrosymmetric space group $P2_1$ (Table 1). Figure 1 displays the unit cell, containing $[(Ph)_3PBr]^+$ cations and pyramidal $[Br_7]^-$ anions. Note that all of the tripodal $[Br_7]^-$ building units

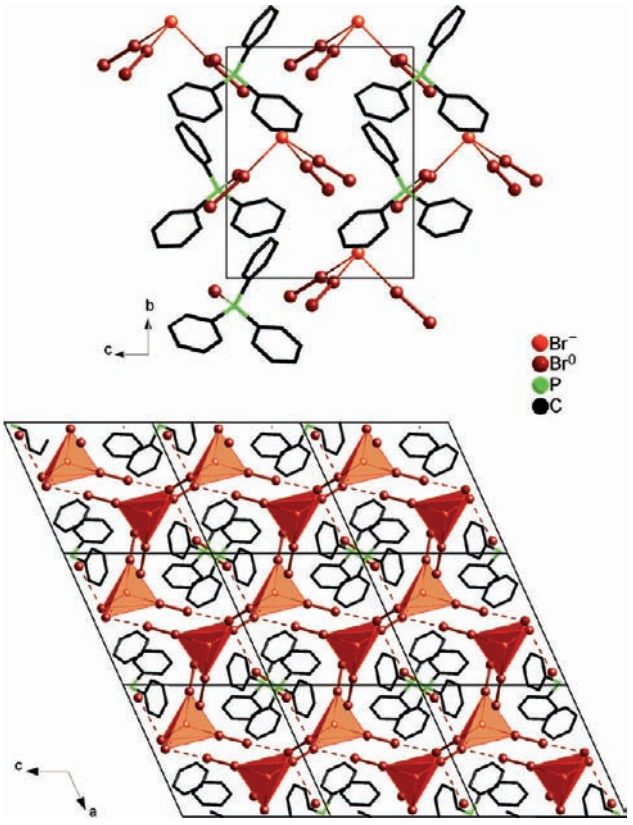

Figure 1. Unit cell of $[(Ph)_3PBr][Br_7]$ showing the unidirectional orientation of the tripodal $[Br_7]^-$ anions and (3 × 3) supercell along the crystallographic (010) direction indicating a 3 + 1 coordination (distorted tetrahedron, light red) around the central bromide anion (Br1) resulting in a polybromide 2D network.

are uniformly oriented with their top along the crystallographic *b* axis. This finding is in good agreement with the absence of a center of inversion as well as with observation of a chiral structure and a polar space group.

At first sight, the Br−Br distances in $[(Ph)_3PBr][Br_7]$ can be categorized in two groups (Table 2). With 233.1−238.1 pm, the shortest distances are observed for three Br_2 units coordinated to the Br atom at the top of the $[Br_7]^-$ pyramid (Figure 2). These Br−Br distances are significantly elongated in comparison to the Br_2 molecule in the solid state (227 pm),[3,4] which points to the influence of additional interactions. The atom representing the top of the $[Br_7]^-$ pyramid can be regarded as a bromide anion and exhibits distances in a range of 287.4−290.7 pm to the three Br_2 units. Thus, the $[Br_7]^-$ anion can be rationalized according to the description $[(Br^-)(Br_2)_3]$. Although unknown as a polybromide anion, such an arrangement is well-known for the polyiodides.[5] For compounds containing $[I_7]^-$ species, such as $[Ph_4P][I_7]$,[38] a composition described by $[(I_3)^-(I_2)_2]$ is, however, much more common. The observed angles at the central Br^- (Br1) and I^- (I1) are finally very similar for $[Br_7]^-$ (83.9−95.7°) as well as for $[I_7]^-$ (85.6−97.3°).

A more detailed consideration of the Br−Br distances shows that extracting an isolated $[Br_7]^-$ is too simplified (Figure 2). In fact, each $[Br_7]^-$ building unit is further connected to four additional $[Br_7]^-$ units via distances of 331.7 (Br1−Br3) and 339.5 (Br3−Br5) pm to form an infinite layer-type arrangement. Moreover, a distance of 349.9 pm (Br2−Br8) between $[Br_7]^-$ and the $[(Ph)_3PBr]^+$

dx.doi.org/10.1021/ic201291k |*Inorg. Chem.* 2011, 50, 11683–11694

Table 2. Comparison of Br−Br Distances of the Polybromides Encountering Distances below the Doubled Van der Waals Radius of Bromine (i.e., 370 pm)

Compound	Br^0-Br^0/pm	$Br^-\cdots(Br_2)$/pm	$(Br_2)\cdots(Br_2)$/pm
Br_2 (solid) [3,4]	*227*	*331 within layers (399 between layers)*	
$[(Ph)_3PBr][Br_7]$	233−238	287−291	332−350
$[(Bz)(Ph)_3P]_2[Br_8]$	231	250−310	360
$[(n\text{-}Bu)_3MeN]_2[Br_{20}]$	231−233	294−314	327−344
$[C_4MPyr]_2[Br_{20}]$	229−234	291−316	325−358

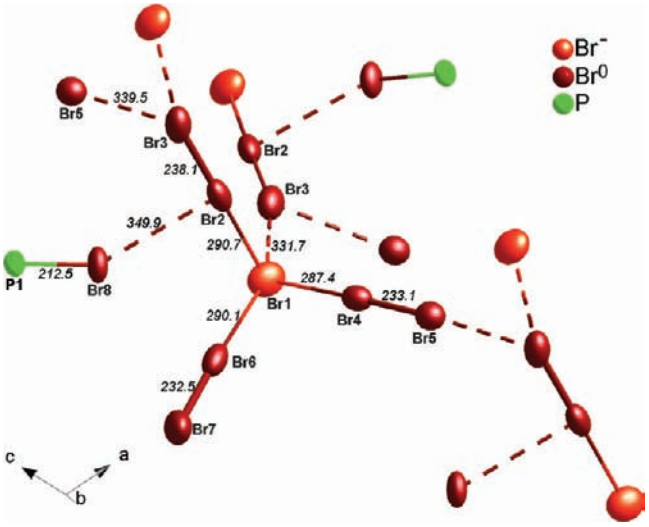

Figure 2. Intra- and intermolecular distances of the $[Br_7]^-$ anion in $[(Ph)_3PBr][Br_7]$ (all distances in pm; thermal ellipsoids with 50% probability of finding).

cation is observed. All of these Br−Br distances range below the doubled van der Waals radius of the element (i.e., 370 pm).[3,4] In summary, the coordination around the central bromide anion (Br1) can also assumed be as 3 + 1 (Figure 1). All four edges of this tetrahedral arrangement show a different connectivity. Hence, two edges of the distorted tetrahedra around Br1 are directly interconnected via a single Br_2 molecule (Br1−Br2−Br3···Br1, Br1···Br3−Br2−Br1), one edge involves two Br_2 molecules (Br1−Br4−Br5···Br3−Br2−Br1), and the final edge (Br1−Br6−Br7) does not exhibit any additional Br−Br interaction at all.

All distances in the $[(Ph)_3PBr]^+$ cation are in accordance with the expectation. As discussed above, the cation is directly involved in the polybromide network via long Br−Br distances. Furthermore, long-ranging charge interaction between the cation and the anionic polybromide naturally occurs. Finally, the shortest Br···H−C interaction is observed with 286.2 pm (to Br8 of the $[(Ph)_3PBr]^+$ cation). With regard to what is discussed as a H−Br bridge bonding (i.e., 240−280 pm),[39−41] a significant influence of such H bridge bonding can be excluded.

With regard to the alternative description of $[(Ph)_3PBr][Br_7]$ either to contain discrete $[Br_7]^-$ anions or an infinite polybromide 2D network, the first view seems much more viable in summary. Thus, the distances inside the $[Br_7]^-$ anion (233−291 pm) are significantly shorter compared to the longer distances to interconnect $[Br_7]^-$ (332−350 pm). This view is also coherent with describing $[(n\text{-}Bu)_3MeN]_2[Br_{20}]$ and $[C_4MPyr]_2[Br_{20}]$ as infinite 2D and 3D networks because the differentiation between

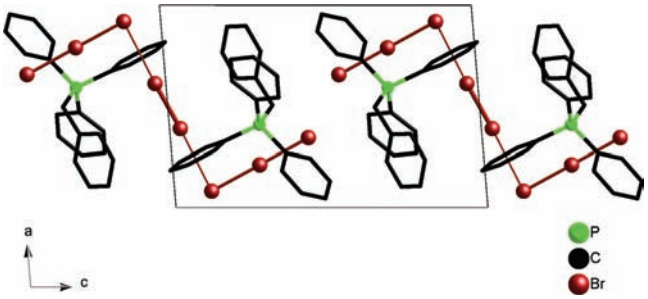

Figure 3. Unit cell of $[(Bz)(Ph)_3P]_2[Br_8]$ with the Z-shaped $[Br_8]^{2-}$ anion.

the shorter first-order and the longer second-order Br−Br distances is much less pronounced compared to that of $[(Ph)_3PBr][Br_7]$.

$[(Bz)(Ph)_3P]_2[Br_8]$. $[(Bz)(Ph)_3P]_2[Br_8]$ was prepared similarly to $[(Ph)_3PBr][Br_7]$ by reacting excess bromine in an equimolar, eutectic mixture of the ionic liquids $[C_{10}MPyr]Br$ and $[C_4MPyr][OTf]$. Instead of $(Ph)_3P$, $[(Bz)(Ph)_3P]Br$ was added here. As a result, light-red crystals of $[(Bz)(Ph)_3P]_2[Br_8]$ were obtained that crystallize triclinically with space group $P\bar{1}$ (Table 1). According to single-crystal structure analysis, the title compound is constituted of $[(Bz)(Ph)_3P]^+$ cations and Z-shaped $[Br_8]^{2-}$ anions (Figure 3).

Although a Z-shaped $[Br_8]^{2-}$ was already observed in the compound $[Q]_2[Br_8]$ (Q = quinuclidinium),[5,10] a direct comparison of the two species, nevertheless, reveals significant differences (Figure 4). First and most obvious, the angle Br2−Br3−Br4 with 88.0° in the title compound is much smaller compared to $[Q]_2[Br_8]$ (i.e., 107°). Consequently, the Z-like shape is more compressed in $[(Bz)(Ph)_3P]_2[Br_8]$. Second, the distances Br1−Br2−Br3 with 251.8 and 249.8 pm in $[(Bz)(Ph)_3P]_2[Br_8]$ are more equalized than those in $[Q]_2[Br_8]$ (i.e., 243 and 266 pm). Thus, the $[Br_8]^{2-}$ anion in $[(Bz)(Ph)_3P]_2[Br_8]$ can be formulated as $[(Br_3^-)_2(Br_2)]$, whereas $[Br_8]^{2-}$ in $[Q]_2[Br_8]$ is better described as $[(Br^-)_2(Br_2)_3]$ (Figure 4). In accordance with this view, the Br−Br distance of the central bromine molecule for both species only shows a minor difference and is slightly shorter in $[(Bz)(Ph)_3P]_2[Br_8]$ than in $[Q]_2[Br_8]$ (i.e., Br4−Br4 with 230.8 vs 235.4 pm; Br4−Br3 with 310.1 vs 317.1 pm). The different conformations of the $[Br_8]^{2-}$ anions in $[(Bz)(Ph)_3P]_2[Br_8]$ and $[Q]_2[Br_8]$, finally, can be attributed to packing effects as well as to the shape and volume of the respective cation. In addition, Br−H bridge bonding has a significant influence. Thus, a remarkably short, and thereby strong, H bridge bonding is observed for $[Q]_2[Br_8]$ (i.e., 239 pm at Br3).[10] In contrast, just comparably weak interactions are observed between $[Br_8]^{2-}$ and $[(Bz)(Ph)_3P]^+$ in the title compound (276.7 and 278.4 pm at Br1; 287.8 pm at Br2).

dx.doi.org/10.1021/ic201291k |*Inorg. Chem.* 2011, 50, 11683–11694

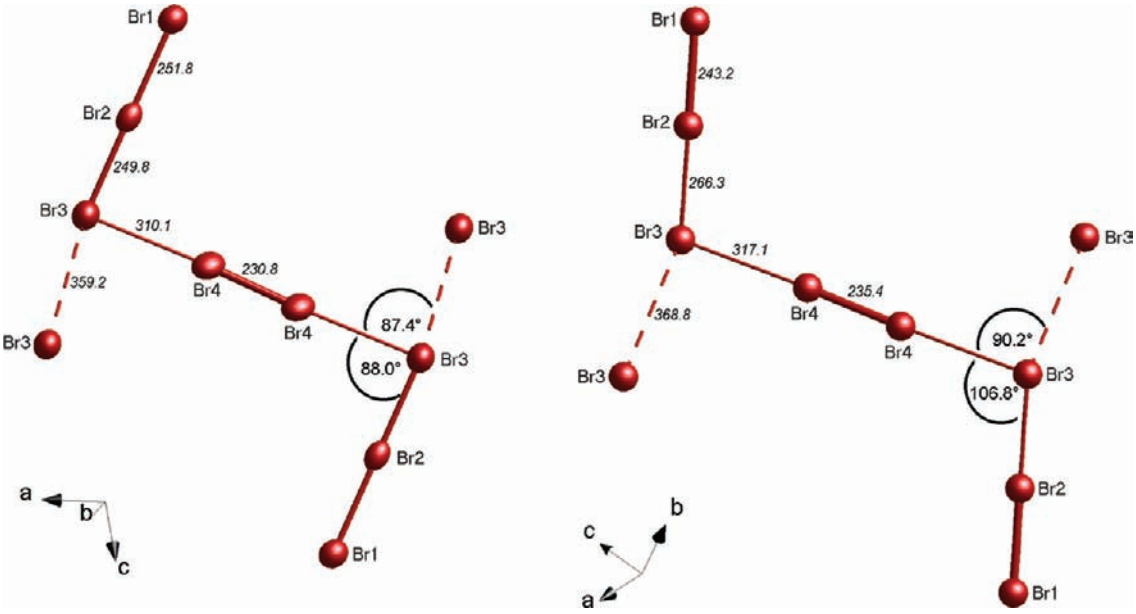

Figure 4. Distances and angles of the $[Br_8]^{2-}$ anion in $[(Bz)(Ph)_3P]_2[Br_8]$ (left) in comparison to $[Q^+]_2[Br_8]$ (right, Q^+ = quinuclidinium)[10] (all distances in pm; thermal ellipsoids with 50% probability).

As discussed for $[(Ph)_3PBr][Br_7]$, second-order Br−Br interactions (Br3−Br3) can be discussed for $[(Bz)(Ph)_3P]_2[Br_8]$ and indicate a tendency of the $[Br_8]^{2-}$ anion to form infinite $^1_\infty[(Br_3^-)_2(Br_2)]$ chains. These second-order distances with 359.2 pm are, however, even longer than those in $[(Ph)_3PBr][Br_7]$. Consequently, extracting a discrete $[Br_8]^{2-}$ anion is even more valuable for $[(Bz)(Ph)_3P]_2[Br_8]$ also.

$[(n\text{-}Bu)_3MeN]_2[Br_{20}]$. $[(n\text{-}Bu)_3MeN]_2[Br_{20}]$ was obtained by reacting an excess of molecular dibromine with $(PhBr)(Ph)_2P$ in $[(n\text{-}Bu)_3MeN][N(Tf)_2]$. While the deep-red crystals melt at about +10 °C, crystal growth was performed by cooling to −15 °C. Suitable single crystals for structure analysis were then selected at about −20 °C. The formation of $[(n\text{-}Bu)_3MeN]_2[Br_{20}]$ can be rationalized to start with proceeding bromination of $(PhBr)(Ph)_2P$, resulting in a slow formation of Br^- anions. On the basis of the alternative description $[(n\text{-}Bu)_3MeN]_2[(Br^-)_2(Br_2)_9]$, the title compound contains an exceptionally high number of nine molecules of dibromine per formula unit.

According to single-crystal structure analysis, $[(n\text{-}Bu)_3MeN]_2[Br_{20}]$ crystallizes monoclinically and, while considering all other polyhalides presented here, with a relatively high space-group symmetry ($C2/c$; Table 1). The compound consists of a central bromide anion (Br1) that is coordinated by five dibromine molecules (Figure 5). As a result, a distorted square-pyramidal coordination with dibromine is obtained. Note that all central bromide anions are equivalent by inversion symmetry. One of the Br_2 molecules (Br9−Br9) serves as a direct linker between two central bromide anions (Figure 6). The remaining four dibromine molecules (Br2−Br3, Br4−Br5, Br6−Br7, and Br8−Br10) also interlink the central bromide (Br1) but in each case involving a second dibromine molecule (Br4−Br5, Br2−Br3, Br2−Br3, and Br9−Br9) that is positioned almost perpendicular to the first. As a consequence, the central Br1 is interconnected by one as well as by two dibromine molecules (Figure 6).

Three different types of Br−Br distances are observed in $[(n\text{-}Bu)_3MeN]_2[Br_{20}]$ (Table 2). The shortest distances (230.9−233.4 pm) represent the dibromine molecules, which are slightly

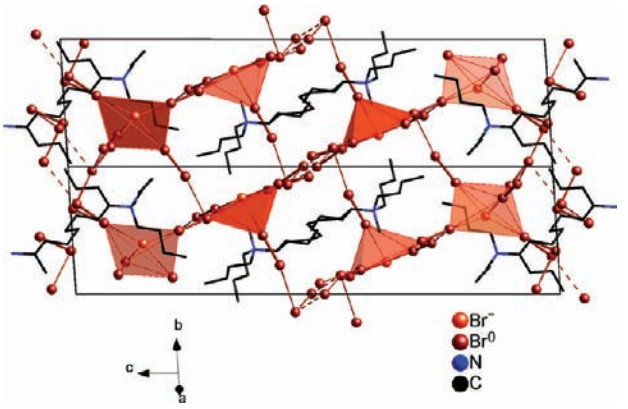

Figure 5. Unit cell of $[(n\text{-}Bu)_3MeN]_2[Br_{20}]$ with the central bromide anion (Br1) coordinated by five dibromine molecules (dark red with bold line) to form distorted square-pyramidal $[Br(Br_2)_5]^-$ building units (foreshadowed in light red) and the $[(n\text{-}Bu)_3MeN]^+$ cation between (disorder of Br5 and the $[(n\text{-}Bu)_3MeN]^+$ cation not shown for clarity).

elongated in comparison to the pure element in the solid state (227 pm).[3,4] Next, the distances between dibromine molecules and the central bromide anion range from 294.3 to 314.2 pm. Finally, distances between 326.5 and 344.4 pm are observed between different dibromine molecules. On the basis of these distances, an infinite layer-type polybromide network is formed that is oriented along the crystallographic *a* and *b* axes (Figure 7). These polybromide layers are further interlinked to each other via Br−Br interactions when including an even longer distance between Br3 and Br5A (364.8 pm). This interaction is still with a distance right below the doubled van der Waals radius of bromine (370 pm)[3,4] (Table 2 and Figure 7).

During structure refinement, a certain disorder was observed for the Br5 atom and tackled by split-atom positions Br5A/Br5B with 50% occupancy for each position (Figure 7). Such disorder

of one or even more halide atoms has been observed for several polyiodides also.[5] Furthermore, the $[NMe(n\text{-}Bu)_3]^+$ cation shows a certain disorder affecting the terminal C atoms of one of the three butyl chains. Such disorder has also often been observed for tetraalkylammonium cations and is here again tackled by split-atom positions with an occupancy of 50%. The relevant butyl chains of two cations in one position of finding are exactly directed in front of each other, which is obviously not possible. In fact, the bonding situation (i.e., H bridge bonding) of the butyl chain as well as the required space in the crystal lattice are more or less identical for both positions of finding. Note that attempts to refine the crystal structure by choosing the noncentrosymmetrical space group *Cc* still involve structural disorder of the cation as well as of Br5, and in addition lead to considerably larger residual values and anisotropic parameters of thermal motion.

At first sight, the $[(n\text{-}Bu)_3MeN]^+$ cation seems to act solely as a kind of template within the polybromide network. A more detailed view, however, indicates significant H bridge bonding involving the disordered Br5 atom (Figure 8). With values of 241.1, 260.2, and 269.5 pm, the observed Br···H−C distances are in a range of what is discussed as a Br−H bridge bonding (240−280 pm; Figure 8).[39−41] In addition, a significantly longer distance is observed between hydrogen and the central bromide anion (Br1···H7A) with 311.4 pm. The latter rather points to a dipole−dipole interaction than to H bridge bonding. Taking the Br1···H7A bonding situation as well as the resulting sterical shielding due to the cation into account, the unusual square-pyramidal $[Br(Br_2)_5]^-$ coordination around the central bromide anion (Br1) can be coherently explained. In addition to H bridge bonding, long-ranging Madelung-type charge interactions between the $[(n\text{-}Bu)_3MeN]^+$ cation and the anionic polybromide network are relevant to the overall bonding and contribute to the stability of the polybromide 2D network.

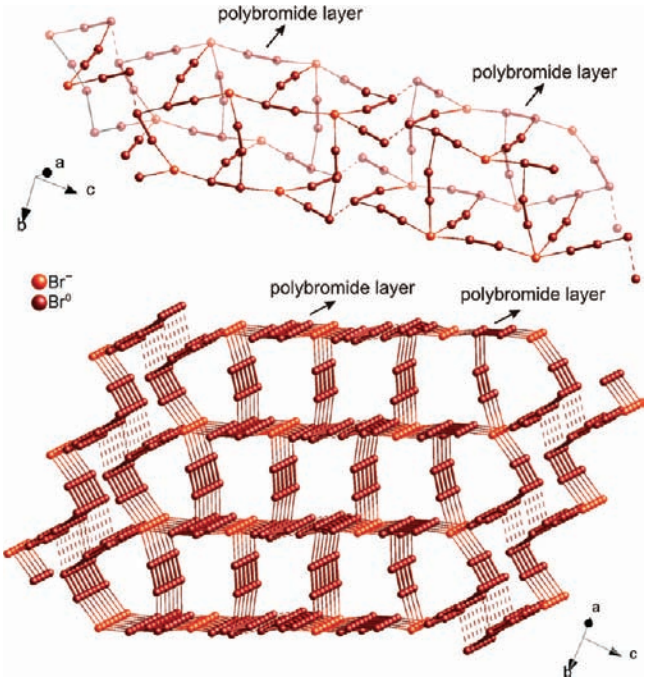

Figure 7. $[(n\text{-}Bu)_3MeN]_2[Br_{20}]$ with $[(Br^-)_3(Br_2)_4(Br_2)_{1/2}]$ and $[(Br^-)_2(Br_2)_4]$ rings that are fused via edge-sharing (top). The resulting polybromide 2D network exhibits layers along the crystallographic (110) direction and a stacking along the *c* axis via longer Br−Br interactions (i.e., 365 pm, dotted lines). The $[(n\text{-}Bu)_3MeN]^+$ cation and disordered Br5 are omitted for clarity.

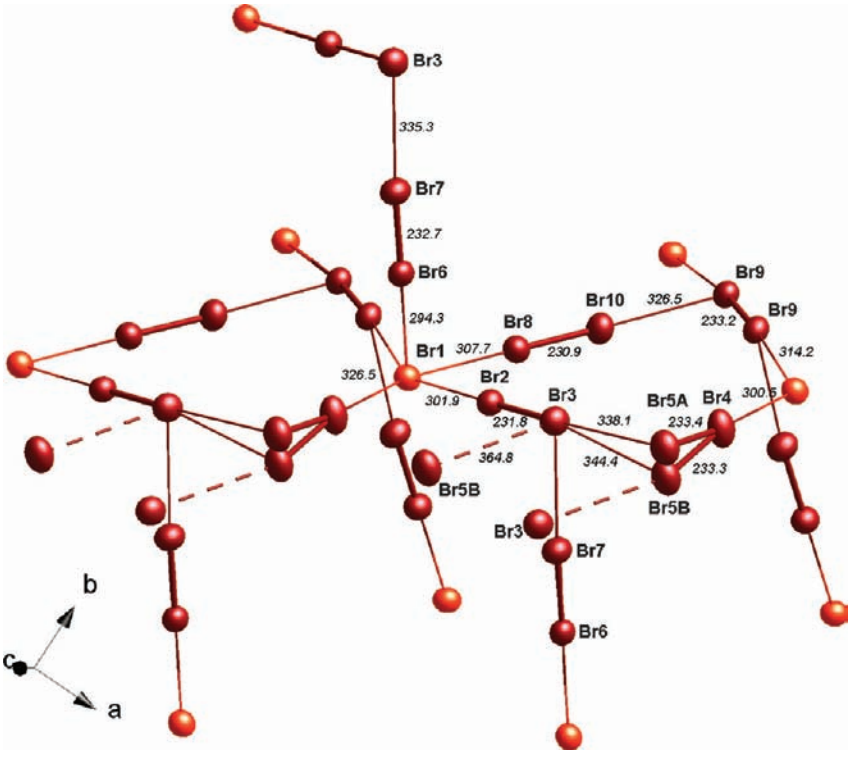

Figure 6. Polybromide 2D network in $[(n\text{-}Bu)_3MeN]_2[Br_{20}]$, with the central bromide anion (Br1: light red) as the network node and the coordinating dibromine molecules (Br_2: dark red) as linkers (all distances in pm; all thermal ellipsoids with 50% probability).

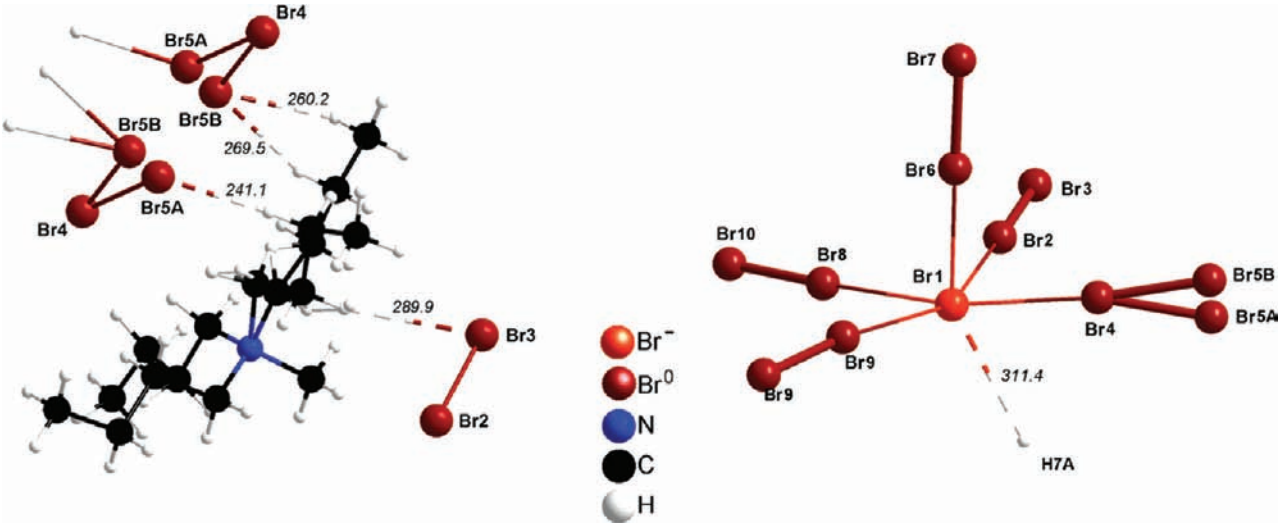

Figure 8. Shortest Br···H−C distances between the bromine network and the $[(n\text{-Bu})_3\text{MeN}]^+$ cation in $[(n\text{-Bu})_3\text{MeN}]_2[\text{Br}_{20}]$ (all distances in pm; all thermal ellipsoids with 50% probability).

The packing of the polybromide network in $[(n\text{-Bu})_3\text{MeN}]_2[\text{Br}_{20}]$ can be described based on the distorted square-pyramidal $[(\text{Br}^-)(\text{Br}_2)_5]$ building unit (Figure 5). Such coordination is rare and has been sparsely observed for the polyiodides also.[5,42] A cross section of the layer-type polybromide illustrates the packing $[(\text{Br}^-)(\text{Br}_2)_5]$ units and reveals an alternative description of the polybromide network (Figure 7). Accordingly, the polybromide layers are directed along the crystallographic (110) direction and stacked along the *c* axis with Br−Br interactions of 365 pm. Each layer is composed of $[(\text{Br}^-)_3(\text{Br}_2)_4(\text{Br}_2)_{1/2}]$ and $[(\text{Br}^-)_2(\text{Br}_2)_4]$ rings that are fused via edge-sharing. In summary, the Br−Br distances in $[(n\text{-Bu})_3\text{MeN}]_2[\text{Br}_{20}]$ with 231−344 pm are much less different from each other compared to $[(\text{Ph})_3\text{PBr}][\text{Br}_7]$ and $[(\text{Bz})(\text{Ph})_3\text{P}]_2[\text{Br}_8]$. In contrast to the discrete anions $[\text{Br}_7]^-$ and $[\text{Br}_8]^{2-}$, this points to the presence of a polybromide 2D network in $[(n\text{-Bu})_3\text{MeN}]_2[\text{Br}_{20}]$.

Polybromides and dibromine-containing compounds, in general, are rare to date. To this concern, the polybromide $[\text{TtddBr}_2]^{2+}[(\text{Br}^-)_2(\text{Br}_2)_3]$ and the bromidometalate $[(\text{C}_4\text{H}_9)_4\text{N}]_2[\text{Pt}_2\text{Br}_{10}](\text{Br}_2)_7$ with six and seven molecules of dibromine per formula unit, to the best of our knowledge, contain the highest percentage of dibromine observed so far.[14,43] Thus, with nine molecules of dibromine, an even higher amount is found in $[(n\text{-Bu})_3\text{MeN}]_2[\text{Br}_{20}]$. Moreover, a comparison with polyiodides is intriguing. Here, $[\text{Fc}]_3\text{I}_{29}$ ([Fc] = ferrocenium) is known as the iodine-richest polyiodide and exhibits the highest halogen-to-halide ratio (i.e., $\text{I}^{\pm0}:\text{I}^{-\text{I}} = 26:3 = 8.67$).[5,6] Hence, $[(n\text{-Bu})_3\text{MeN}]_2[\text{Br}_{20}]$ with a $\text{Br}^{\pm0}:\text{Br}^{-\text{I}}$ ratio of 18:2 = 9.00 contains even more of the elemental halogen than the iodine-richest polyiodide.

Because large quantities of $[(n\text{-Bu})_3\text{MeN}]_2[\text{Br}_{20}]$ could be obtained, the thermal stability of the compound was studied. According to TG, decomposition occurs with three steps (Figure 9): (a) 40−200 °C (−40.0%), (b) 200−220 °C (−24.0%), and (c) 220−340 °C (−30.6%). These steps can be rationalized based on the following decomposition products: (a) 5Br_2 (calcd −40.0%), (b) 6HBr (calcd −24.3%), and (c) $2(\text{C}_4\text{H}_8\text{Br})_2(\text{C}_4\text{H}_9)(\text{CH}_3)\text{N}$ (calcd −35.7%). Although several reactions may partly occur in parallel (e.g., evaporation of dibromine, radical bromination, evaporation of HBr, fragmentation of the $[(n\text{-Bu})_3\text{MeN}]^+$ cation), the thermal decomposition can, nevertheless, be quantified in detail. Note that minor amounts of black carbon remain inside the crucible subsequent to TG. The overall good agreement between the experiment and calculation finally evidences the phase purity of $[(n\text{-Bu})_3\text{MeN}]_2[\text{Br}_{20}]$ and its successful separation from the ionic liquid.

$[\text{C}_4\text{MPyr}]_2[\text{Br}_{20}]$. A composition very comparable to that of $[(n\text{-Bu})_3\text{MeN}]_2[\text{Br}_{20}]$ was obtained with $[\text{C}_4\text{MPyr}]_2[\text{Br}_{20}]$.[27] At first glance, just the cation was exchanged and led to a second compound, again containing a remarkable number of nine molecules of dibromine ($[\text{C}_4\text{MPyr}]_2[(\text{Br}^-)_2(\text{Br}_2)_9]$). Together, $[(n\text{-Bu})_3\text{MeN}]_2[\text{Br}_{20}]$ and $[\text{C}_4\text{MPyr}]_2[\text{Br}_{20}]$ contain the highest percentage of dibromine ever observed and exhibit an even higher $\text{X}^{\pm0}:\text{X}^{-\text{I}}$ ratio as the iodine-richest polyiodide $(\text{Fc})_3\text{I}_{29}$.[5,6] In contrast to $[(n\text{-Bu})_3\text{MeN}]_2[\text{Br}_{20}]$, $[\text{C}_4\text{MPyr}]_2[\text{Br}_{20}]$ is, however, with a significantly different structural arrangement and connectivity of the Br atoms.

$[\text{C}_4\text{MPyr}]_2[\text{Br}_{20}]$ was gained in yields of 80% by dissolving elemental bromine in an equimolar mixture of the ionic liquids $[\text{C}_{10}\text{MPyr}]\text{Br}$ and $[\text{C}_4\text{MPyr}]\text{OTf}$. Note that the deep-red, highly adhesive crystals melt at about +9 °C. $[\text{C}_4\text{MPyr}]_2[\text{Br}_{20}]$ crystallizes triclinically with space group $P\bar{1}$ (Table 1). Its central building unit is, similar to $[(n\text{-Bu})_3\text{MeN}]_2[\text{Br}_{20}]$, a bromide anion (Br1; Figure 10). Again, all central bromide anions are equivalent by inversion symmetry. In contrast to $[(n\text{-Bu})_3\text{MeN}]_2[\text{Br}_{20}]$, the central bromide anion in $[\text{C}_4\text{MPyr}]_2[\text{Br}_{20}]$ is, however, coordinated by six dibromine molecules. Four of these Br_2 molecules (Br2−Br2, Br7−Br8, Br8−Br7, and Br9−Br9) directly interlink the bromide anion (Br1). The remaining two dibromine molecules (Br3−Br4 and Br5−Br6) also serve as linkers but in each case involving a second dibromine molecule (Br5−Br6 and Br7−Br8), positioned almost perpendicular to the first one. Thus, Br1 is interconnected four times via two Br atoms, once via three (Br1−Br5−Br6···Br7−Br1) and once via four (Br1−Br3−Br4···Br6−Br5−Br1) Br atoms (Figure 10). In addition, a ninth dibromine molecule (Br10−Br10) is not coordinated to the central bromide anion (Br1) but only to Br8.

Again, the Br−Br distances in $[\text{C}_4\text{MPyr}]_2[\text{Br}_{20}]$ can be differentiated into three groups (Table 2 and Figure 10). The shortest distances (229−234 pm) stem from dibromine molecules that are slightly longer than those observed for the pure

dx.doi.org/10.1021/ic201291k |*Inorg. Chem.* 2011, 50, 11683–11694

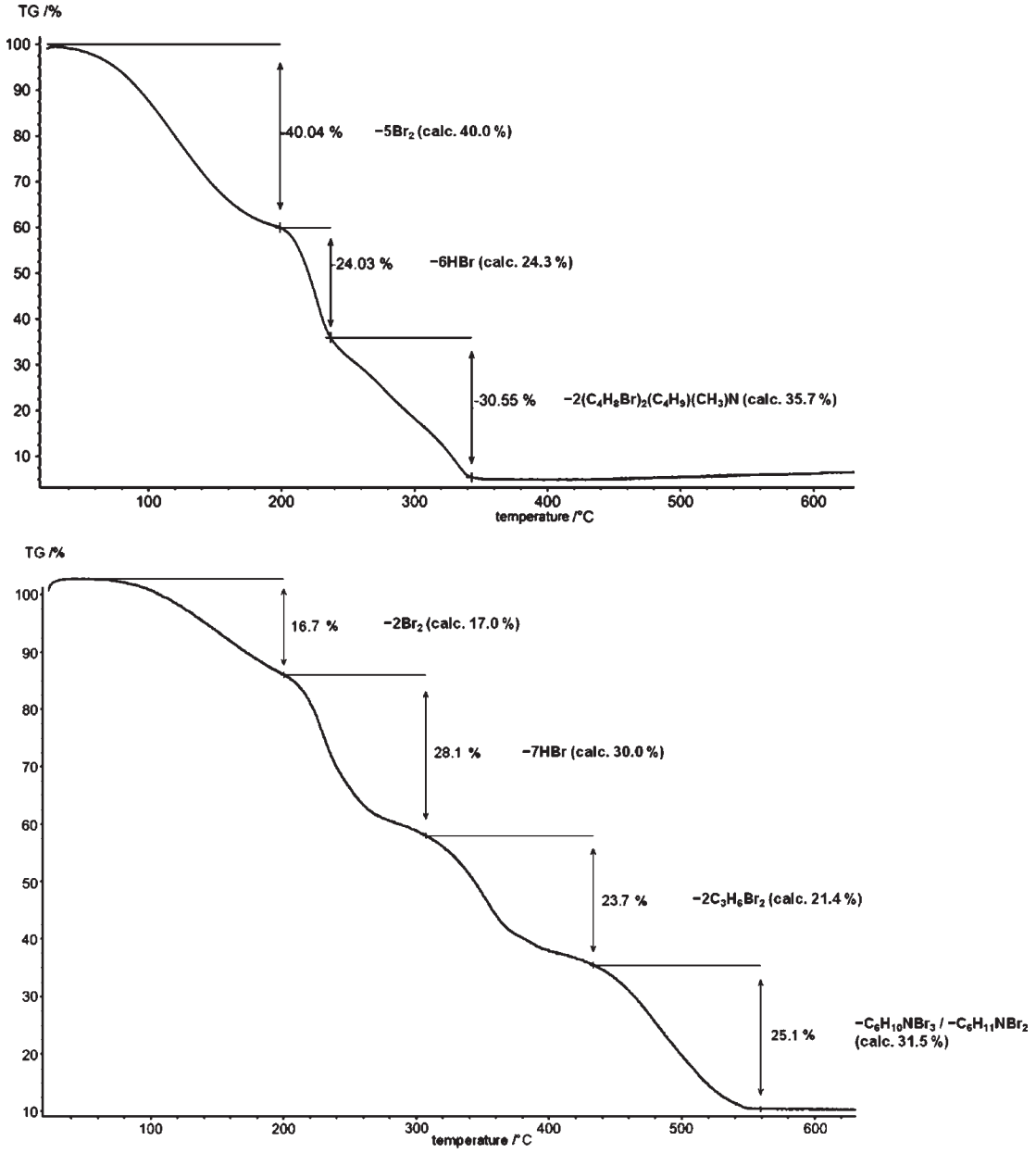

Figure 9. TG of $[(n\text{-Bu})_3\text{MeN}]_2[\text{Br}_{20}]$ (top) and $[\text{C}_4\text{MPyr}]_2[\text{Br}_{20}]$ (bottom) indicating three- and four-step weight losses at 40−340 and 60−560 °C.

element in the solid state (227 pm).[3,4] Next, distances between dibromine molecules and the central bromide anion range from 291 to 316 pm. Even longer distances between 325 and 358 pm are finally observed between different dibromine molecules. Again, the difference in length between these Br−Br distances is much less distinctive compared to the clear gap between shorter first-order and longer second-order distances in $[(\text{Ph})_3\text{PBr}][\text{Br}_7]$ and $[(\text{Bz})(\text{Ph})_3\text{P}]_2[\text{Br}_8]$. Consequently, describing $[\text{C}_4\text{MPyr}]_2[\text{Br}_{20}]$ as a $^3_\infty[(\text{Br}^-)_2(\text{Br}_2)_9]$ 3D network is much more meaningful than any extraction of an isolated building unit. Remarkably, the bromine network in $[\text{C}_4\text{MPyr}]_2[\text{Br}_{20}]$ is established without involving any other element than bromine and represents the first polybromide 3D network that is exclusively established via interaction of bromine. Structurally, the bromine network in $[\text{C}_4\text{MPyr}]_2[\text{Br}_{20}]$ can be rationalized based on distorted, corner-sharing $[(\text{Br}^-)(\text{Br}_2)_4(2\text{Br}_2)_2]^-$ octahedra (Figure 11). As a result, a $^3_\infty[(\text{Br}^-)_2(\text{Br}_2)_4(2\text{Br}_2)_2(\text{Br}_2)]$ network is obtained that is closely related to the CsCl type of structure. This becomes obvious when reckoning the $[\text{C}_4\text{MPyr}]^+$ cation as coordinated by eight $[(\text{Br}^-)(\text{Br}_2)_4(2\text{Br}_2)_2]^-$ building units and vice versa (Figure 10).

For $[\text{C}_4\text{MPyr}]_2[\text{Br}_{20}]$, even the shortest Br···H−C distance (292 pm) ranges above typical values of Br−H bridge bonding (240−280 pm).[39−41] In contrast to $[(n\text{-Bu})_3\text{MeN}]_2[\text{Br}_{20}]$, the $[\text{C}_4\text{MPyr}]^+$ cation can, therefore, be considered as more or less "naked". In addition to its template-like function, long-ranging Madelung-type charge interaction between $[\text{C}_4\text{MPyr}]^+$ and the anionic network is naturely relevant to the overall stability of the 3D polybromide. According to TG (Figure 9), $[\text{C}_4\text{MPyr}]_2[\text{Br}_{20}]$ decomposes with four steps up to a temperature of 550 °C, including (a) 60−190 °C (−16.7%), (b) 190−290 °C (−28.1%), (c) 290−420 °C (−23.7%), and (d) 420−550 °C (−25.1%).[27]

dx.doi.org/10.1021/ic201291k |*Inorg. Chem.* 2011, 50, 11683–11694

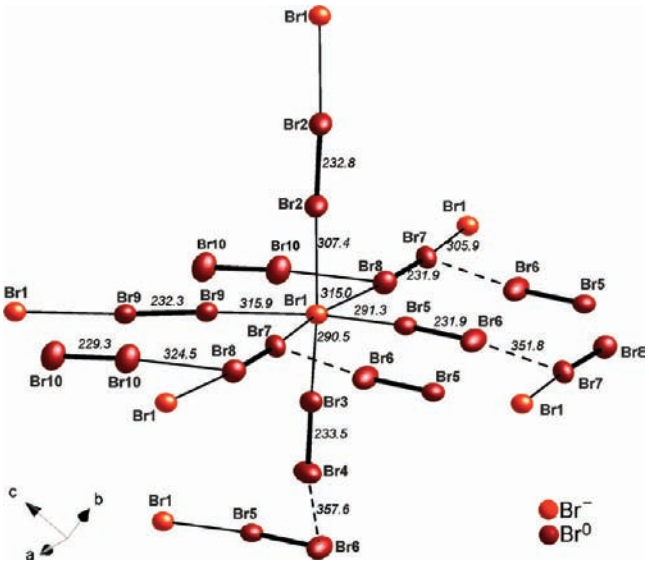

Figure 10. $[C_4MPyr]_2[Br_{20}]$ with the central bromide anion (Br1, light red) as the network node with coordinating dibromine molecules (Br_2, dark red) as linkers (all Br−Br distances in pm; all thermal ellipsoids with 50% probability).

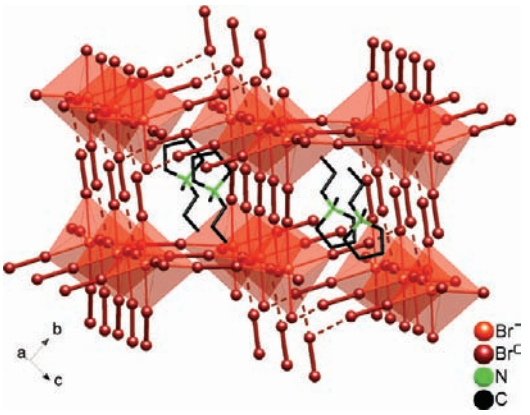

Figure 11. $^3_\infty[(Br^-)_2(Br_2)_4(2Br_2)_2(Br_2)]$ network in $[C_4MPyr]_2[Br_{20}]$ established by distorted corner-sharing $[(Br^-)(Br_2)_4(2Br_2)_2]^-$ octahedra (foreshadowed in light red) with the central bromide anion (Br1) as the network node that is interlinked by dibromine molecules (dark red with bold line). The $[C_4MPyr]^+$ cation serves as a template between layers of the polybromide 3D network.

These values can be ascribed to a loss of (a) $2Br_2$ (calcd −17.0%), (b) 7HBr (calcd −30.0%), (c) $2C_3H_6Br_2$ (calcd −21.4%), and (d) $C_6H_{10}NBr_3/C_6H_{11}NBr_2$ (calcd −31.5%). The reliable quantification as well as the clear differentiation between the thermal decomposition of $[(n\text{-}Bu)_3MeN]_2[Br_{20}]$ and $[C_4MPyr]_2[Br_{20}]$ again points to the phase purity of both bromine-rich compounds. In this context, the different temperatures for complete decomposition (i.e., 340 °C for $[(n\text{-}Bu)_3MeN]_2[Br_{20}]$ and 560 °C for $[C_4MPyr]_2[Br_{20}]$) can be related to the different stabilities of the respective cation. The slightly higher onset of the bromine release (i.e., 40 °C for $[(n\text{-}Bu)_3MeN]_2[Br_{20}]$ and 60 °C for $[C_4MPyr]_2[Br_{20}]$), on the other hand, indicates a higher stability of the polybromide 3D network compared to the 2D network.

Considering the melting point and vapor pressure of elemental bromine, the infinite bromine-rich networks in $[(n\text{-}Bu)_3MeN]_2[Br_{20}]$ and $[C_4MPyr]_2[Br_{20}]$ turn out to be surprisingly stable. While each single Br−Br bond is weak, this finding has to be attributed to the manifold of Br−Br interactions that are almost isotropically spread over the volume of the unit cell. Attempts to further verify the Br−Br bonding situation via Raman spectroscopy or quantum-chemical calculations have failed so far. In contrast to very recent reports on Raman spectra of small, discrete polybromide species (i.e., $[Br_n]^-$ with $n \leq 10$),[44] $[(n\text{-}Bu)_3MeN]_2[Br_{20}]$ and $[C_4MPyr]_2[Br_{20}]$ exhibit just a broad, irregular-shaped absorption between 300 and 100 cm^{-1}. This finding is to be expected in view of the huge number of very similar Br−Br interactions inside the infinite network. In addition, performing quantum-chemical calculations is definitely more than routine with regard to the restrictions of the concrete compounds, viz., multielectron systems, low space-group symmetry, infinite 3D networks, high polarizability of each Br atom as well as the huge number of largely similar, comparably weak halogen−halogen interactions. Even for the long-known polyiodides, only a few quantum-chemical calculations are available by now. Here, the structure of "small" polyiodides ($[I_n]^-$ with $n \leq 10$) is still part of a controversial discussion.[5−8,13,14] Note that the first quantum-chemical calculations for "small" polybromides have been reported quite recently.[44]

$[(Ph)_3PCl]_2[Cl_2I_{14}]$. While the synthesis in ionic liquids yielded a variety of novel polybromide species, a straightforward extension is to replace Br_2 by the homologous lighter and heavier halogen, viz., iodine monochloride (ICl). Knowledge on polyiodine chlorides is rare to date and limited to small discrete anions. Here, the linear trihalide with its isomers $[Cl-I-Cl]^-$, $[I-I-Cl]^-$, and $[I-Cl-I]^-$ has been frequently described.[45−47] A crystal structure analysis of $[Cl-Cl-I]^-$ is, however, still lacking. Ab initio molecular orbital studies concerning the stability of the mixed trihalide anions $[X_2Y]^-$ in the gas phase and in solution validate the isomers $[X-Y-X]^-$ and $[Y-Y-X]^-$ to be more stable than $[Y-X-X]^-$ and $[Y-X-Y]^-$ if Y is heavier than X.[48,49] Moreover, $[Cl-I-I-Cl]^{2-}$ as a linear anion and $[Cl-I-Cl-I-Cl]^-$ as a V-shaped anion were crystallographically characterized.[50,51] A single infinite chainlike $[I_2Cl]^-$ was reported for $[(PhenH)^+]_2[(I_2Cl)^-(ICl_2)^-]$ [PhenH = bis(1,10-phenanthrolin-1-ium].[46] Finally, the square-planar $[ICl_4]^-$ has been known for many years but is still part of a versatile discussion addressing crystal structure, phase transitions, nuclear quadrupole resonance spectroscopy, and measurements of the heat capacity and dielectric properties.[52−54]

With a strategy that is very similar to the synthesis of polybromides, $[(Ph)_3PCl]_2[Cl_2I_{14}]$ is now obtained as the first polyiodine chloride 3D network. In concrete, excess iodine monochloride was reacted with $(Ph_3)P$ in $[C_4MPyr][OTf]$ as the ionic liquid and resulted in deep-red, plate-shaped crystals exhibiting the monoclinic space group $P2_1/c$ (Table 1). According to the alternative description $[(Ph)_3PCl]_2[(Cl^-)_2(I_2)_7]$, a central chloride anion (Cl2) is here coordinated by five molecules of diiodine (Figure 12). Four of these I_2 molecules (I1−I2, I3−I4, I2−I1, and I4−I3) directly interconnect the central chloride anions (Cl2) that are crystallographically identical because of inversion symmetry. As a result, a polyiodine chloride 2D network is formed. The remaining disordered diiodine molecule ($I5_{A/B}-I6_{A/B}$) interlinks such a layer to similar layers above and below. Interlinking to the next central Cl2 anion here involves an additional diiodine molecule, which is arranged almost perpendicular to $I5_{A/B}-I6_{A/B}$. Besides the square-pyramidal coordination with diiodine around the central chloride anion, an additional diiodine molecule (I7−I7) interlinks the polyiodine chloride layers via I1 (I1···I7−I7···I1).

dx.doi.org/10.1021/ic201291k |*Inorg. Chem.* 2011, 50, 11683–11694

All Cl−I distances with 301.2−309.3 pm are in a very similar range. Extracting a discrete polyhalide anion is, therefore, not meaningful. Thus, the central chloride anion (Cl2) can rather be regarded as a network node that is interlinked by diiodine molecules as a linker to form a 2D network. Herein, square-pyramidal $[Cl(I_{2/1})(I_{2/2})_4]^-$ building units are arranged via corner-sharing to form layers along the crystallographic *bc* plane (Figure 13). Noteworthy, the top of the $[Cl(I_{2/1})(I_{2/2})_4]^-$ pyramids alternates to [100] and $[\bar{1}00]$ along the *b* axis, whereas all pyramids are directed to [100] along the *c* axis. Comparing the mean Cl−I distance of 305.5 pm in $[(Ph)_3PCl]_2[Cl_2I_{14}]$ to polyhalides containing related Cl−I−I building units is illustrative. Thus, two groups of Cl−I bonds become obvious. The first group is represented by an isolated trihalide $[Cl-I-I]^-$ exhibiting a comparably short Cl−I distance of 274.9 pm.[47] In $[(PhenH)^+]_2[(I_2Cl)^-(ICl_2)^-]$, in contrast, the $[Cl-I-I]^-$ building units are interlinked by long-ranging contacts to form infinite chains. This interlinking results in an attenuation of the initial Cl−I bond and significantly longer distances of 304 and 316 pm.[46] Such a situation has been also observed for the anion $[Cl-I-I-Cl]^{2-}$ with a Cl−I distance of 307 pm.[50] Here, strong Cl−H bonds are involved and result in a network via H bridge bonding. Altogether, the Cl−I bonding situation in $[(Ph)_3PCl]_2[Cl_2I_{14}]$ is well in accordance with the above literature data and points to the presence of an infinite polyiodine chloride network.

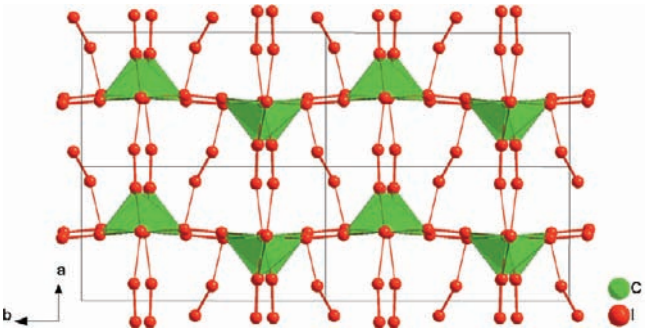

Figure 12. 2 × 2 super cell of $[P(Ph)_3Cl]_2[Cl_2I_{14}]$ with square-pyramidal coordination (green) around the central chloride anion ($[P(Ph)_3Cl]^+$ cation omitted for clarity).

As discussed above, the observed $^2_\infty[Cl(I_{2/1})(I_{2/2})_4]^-$ polyiodine chloride network is, furthermore, interconnected along the *a* axis via two types of diiodine molecules ($I5_{A/B}-I6_{A/B}$ and I7−I7) to form a 3D network. The layers are displaced by the length of a Cl−I bond (approximately 300 pm) along the *c* axis (Figure 13). As a result, the diodine molecule ($I5_{A/B}-I6_{A/B}$) is coordinated, on the one hand, to the central chloride anion (Cl2) and, on the other hand, to I3 in layers positioned above and below. The diodine molecule (I7−I7) is not in contact to the central chloride but only connected to I1 in one layer and I2 in layers above or below. The intermolecular I−I distances (I1−I7 = 359.4 pm) are quite strong compared to typical values (i.e., 360−420 pm)[5] and significantly shorter than the doubled van der Waals radius of iodine (420 pm).[3,4] Hence, the I1···I7−I7···I1 interaction connects the $^2_\infty[Cl(I_{2/1})(I_{2/2})_4]^-$ layers along the *a* axis and plays a major role with regard to the formation of the 3D network. Considerably longer distances are observed in addition for $I6_{A/B}\cdots I3$ (377.0 and 394.7 pm). Note that the latter interaction is not essential with regard to the polyiodine chloride 3D network.

With concern to the $[P(Ph)_3Cl]^+$ cation, again the question arises whether any H bridge bonding occurs in the polyiodine chloride network. With 294.4 pm, the shortest Cl···H distance is here observed inside the cation (Cl1···H6; Figure 14). All additional Cl−H contacts are considerably longer than the sum of the van der Waals radii (Cl = 175 pm; H = 120 pm). On the

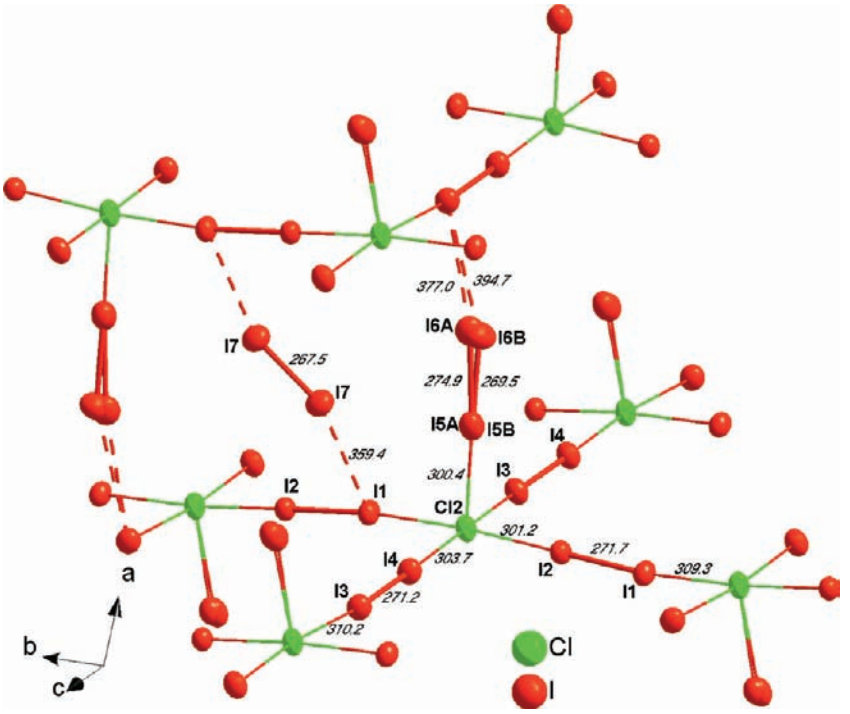

Figure 13. $[P(Ph)_3Cl]_2[Cl_2I_{14}]$ with the central chloride anion (Cl2, green) as the network node and coordinating diiodine molecules (I_2, orange) as linkers (all distances in pm; all thermal ellipsoids with 50% probability).

dx.doi.org/10.1021/ic201291k |*Inorg. Chem.* 2011, 50, 11683–11694

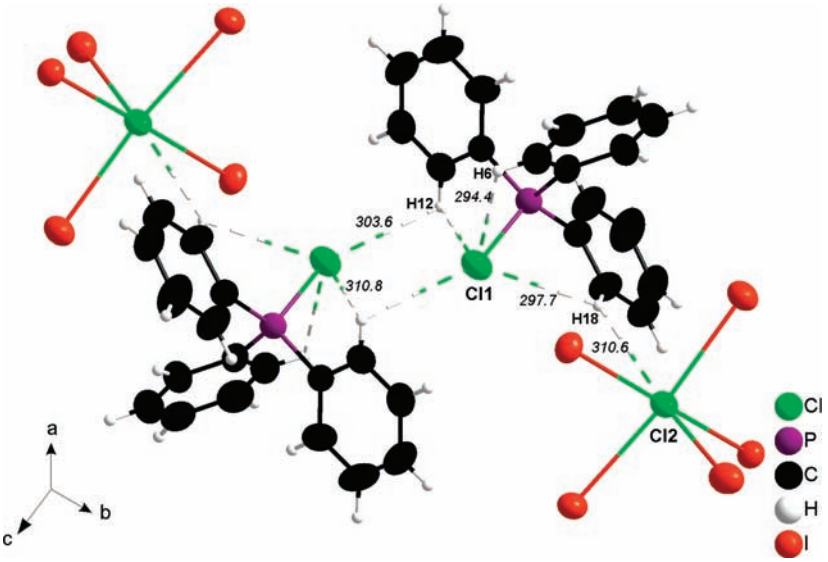

Figure 14. Shortest Cl···H−C distances between the polyiondine chloride network and the $[PPh_3Cl]^+$ cation in $[P(Ph)_3Cl]_2[Cl_2I_{14}]$ (disorder of I5A/I5B omitted for clarity; all distances in pm; all thermal ellipsoids with 50% probability).

other hand, the distance between Cl2 and H18 (310.6 pm) has to be considered in more detail. Although this value is far above of a H bridge bonding, the spatial vicinity between the central chloride anion and the cation becomes obvious. On the basis of this situation, the uncommon square-pyramidal coordination of the $[Cl(I_{2/1})(I_{2/2})_4]^-$ building unit can be rationalized similarly to the case of $[(n\text{-}Bu)_3MeN]_2[Br_{20}]$. All distances of the $[P(Ph)_3Cl]^+$ cation, finally, are well in agreement with the expectation.

CONCLUSION

The chemistry of the halogens is extended by the four novel polybromides $[(Ph)_3PBr][Br_7]$, $[(Bz)(Ph)_3P]_2[Br_8]$, $[(n\text{-}Bu)_3MeN]_2[Br_{20}]$, and $[C_4MPyr]_2[Br_{20}]$. Hereof, $[(n\text{-}Bu)_3MeN]_2[Br_{20}]$ and $[C_4MPyr]_2[Br_{20}]$ represent infinite 2D and 3D networks, containing the highest percentage of dibromine and elemental halogen ever observed. $[(Ph)_3PCl]_2[Cl_2I_{14}]$ consists of an infinite halogen network also and represents the first example of a polyiodine chloride 3D network. All compounds are accessible by a surprisingly facile synthesis in ionic liquids. These solvents, on the one hand, are stable against the strongly oxidizing starting materials Br_2 and ICl. On the other hand, ionic liquids reduce the volatility of the elemental halogens and thereby allow a straightforward excess to halogen-rich compounds.

Despite of almost 100 years of research on halogens and polyhalides, the ionic-liquid-based approach allows one to extend the horizon to a wide range of novel compounds, especially in view of halogen-rich polyhalides. While just an exchange of the cation results in new polybromide networks (i.e., $[(n\text{-}Bu)_3MeN]_2[Br_{20}]$, $[C_4MPyr]_2[Br_{20}]$), one may expect many more polyhalides and halogen-rich compounds from the ionic-liquid-based approach. Although each single halogen−halogen interaction is weak, the manifold of interactions that are largely isotropically arranged inside the infinite networks can be regarded as an important feature in view of the stability of the polybromides. Another important issue is related to the long-ranging Madelung-type charge interaction between the spacious cation and the anionic polyhalide network. Quantum-chemical calculations could by highly interesting to verify the bonding situation. With regard to infinite networks of the highly polarizable halogens and the manifold of very similar, but weak interactions, such calculations will, however, be a challenge. With regard to application, the newly discovered halogen-rich polybromide and polyiodine chloride networks could be interesting for saving storage and handling the reactive halogens and interhalogens. Moreover, the compounds might be relevant for future high-power batteries.

ASSOCIATED CONTENT

Supporting Information. X-ray crystallographic data in CIF format. This material is available free of charge via the Internet at http://pubs.acs.org.

AUTHOR INFORMATION

Corresponding Author
*E-mail: claus.feldmann@kit.edu.

ACKNOWLEDGMENT

The authors are grateful to the Center for Functional Nanostructures of the Deutsche Forschungsgemeinschaft at the KIT for financial support.

REFERENCES

(1) Jörgensen, S. M. *J. Prakt. Chem.* **1871**, *3*, 328–349.
(2) Mooney, R. C. L. *Z. Kristallogr.* **1935**, *90*, 143–150.
(3) Shriver, D.; Atkins, P. *Inorganic Chemistry*; Oxford Textbooks: London, 2006.
(4) Hollemann, A. F.; Wiberg, N. *Lehrbuch der Anorganischen Chemie*; de Gruyter: Berlin, 2007.
(5) Svenson, P. H.; Kloo, L. *Chem. Rev.* **2003**, *103*, 1649–1684.
(6) Tebbe, K. F.; Buchem, R. *Angew. Chem.* **1997**, *36*, 1345–1346. *Angew. Chem., Int. Ed.* **1997**, *36*, 1345–1346.
(7) Tebbe, K. F.; Buchem, R. *Eur. J. Inorg. Chem.* **2000**, *6*, 1275–1282.
(8) Menon, S.; Rajasekharan, M. V. *Inorg. Chem.* **1997**, *36*, 4983–4987.
(9) Stromme, K. O. *Acta Chem. Scand.* **1959**, *13*, 2089–2100.

(10) Robertson, K. N.; Bakshi, P. K.; Cameron, T. S.; Knop, O. *Z. Anorg. Allg. Chem.* **1997**, *623*, 104–114.
(11) Cunningham, C. W.; Burns, G. R.; McKee, V. *Inorg. Chim. Acta* **1990**, *167*, 135–137.
(12) Bricklebank, N.; Skabara, P. J.; Hibbs, D. E.; Hurstouse, M. B.; Malik, K. M. A. *J. Chem. Soc., Dalton Trans.* **1999**, 3007–3013.
(13) Aragoni, M. C.; Arca, M.; Devillanova, F. A.; Hursthouse, M. B.; Huth, S. L.; Isaia, F.; Lippolis, V.; Mancini, A.; Ogilvie, H. *Inorg. Chem. Commun.* **2005**, *8*, 79–82.
(14) Aragoni, M. C.; Arca, M.; Devillanova, F. A.; Isaia, F.; Lippolis, V.; Mancini, A.; Pala, L.; Slawin, A. M. Z.; Woollins, J. D. *Chem. Commun.* **2003**, 2226–2227.
(15) Taraba, J.; Zak, Z. *Inorg. Chem.* **2003**, *42*, 3591–3594.
(16) Riedel, S.; Köchner, T.; Wang, X.; Andrews, L. *Inorg. Chem.* **2010**, *49*, 7156–7164.
(17) Braida, B.; Hiberty, P. C. *J. Am. Chem. Soc.* **2004**, *126*, 14890–14898.
(18) Christian, G. D. *Analytical Chemistry*; Wiley: New York, 2003.
(19) Grätzel, M. *Prog. Photovolt.* **2006**, *14*, 429–442.
(20) Fabjan, C.; Drobits, J. In *Handbook of Battery Materials*; Besenhard, J. O., Ed.; Wiley-VCH: Weinheim, Germany, 1999; pp 177−194.
(21) Khan, M. D.; Majibur, R.; Gotoh, Y.; Morikawa, H.; Miura, M. *Textile Res. J.* **2009**, *79*, 1305–1311.
(22) Mora, M.; Jimenez-Sanchidrian, C.; Ruiz, J. R. *Appl. Organomet. Chem.* **2008**, *22*, 122–127.
(23) Ceccon, A.; Crociani, L.; Santi, S.; Venzo, A.; Biffis, A.; Boccaletti, G. *Tetrahedron Lett.* **2002**, *43*, 8475–8478.
(24) Kautek, W.; Conradi, A.; Sahre, M.; Fabjan, Ch.; Drobits, J.; Bauer, G.; Schuster, P. *J. Electrochem. Soc.* **1999**, *146*, 3211–3216.
(25) Getsis, A.; Mudring, A. V. *Z. Anorg. Allg. Chem.* **2009**, *635*, 2214–2221.
(26) MacFarlane, D. R.; Meakin, P.; Sun, J.; Amini, N.; Forsyth, N. *J. Phys. Chem. B* **1999**, *103*, 4164–4170.
(27) Wolff, M.; Meyer, J.; Feldmann, C. *Angew. Chem., Int. Ed.* **2011**, *50*, 4970–4973.
(28) Wasserscheid, P., Welton, T., Eds. *Ionic Liquids in Synthesis*; Wiley-VCH: Weinheim, Germany, 2008.
(29) Krossing, I.; Slattery, J. M.; Daguenet, C.; Dyson, P. J. *J. Am. Chem. Soc.* **2006**, *128*, 13427–13434.
(30) Giernoth, R. *Angew. Chem.* **2010**, *122*, 2896–2300. *Angew. Chem., Int. Ed.* **2010**, *49*, 2834–2839.
(31) Guloy, A. M.; Ramlau, R.; Tang, Z.; Schnelle, W.; Braitinger, M.; Grin, Y. *Nature* **2006**, *443*, 320–323.
(32) Santiso-Quinones, G.; Brückner, R.; Knapp, C.; Dionne, I.; Passmore, J.; Krossing, I. *Angew. Chem.* **2009**, *121*, 1153–1157. *Angew. Chem., Int. Ed.* **2009**, *48*, 1133–1137.
(33) Biswas, K.; Zhang, Q.; Chung, I.; Song, J. H.; Androulakis, J.; Freeman, A. J.; Kanatzidis, M. G. *J. Am. Chem. Soc.* **2010**, *32*, 14760–14762.
(34) Xie, T.; Brockner, W.; Gjikaj, M. *Z. Anorg. Allg. Chem.* **2010**, *636*, 2633–2640.
(35) Kanatani, A.; Matsumoto, K.; Hagiwara, R. *Eur. J. Inorg. Chem.* **2010**, 1049–1055.
(36) Deetlefs, M.; Hussey, C. L.; Mohammed, T. J.; Seddon, K. R.; van den Berg, J. A.; Zora, J. A. *Dalton Trans.* **2006**, 2334–2341.
(37) Babai, A.; Mudring, A. V. *Inorg. Chem.* **2005**, *44*, 8168–8169.
(38) Poli, G.; Gordon, J. C.; Khanna, R. K.; Fanwick, P. S. *Inorg. Chem.* **1992**, *31*, 3165–3167.
(39) Ozeryanskii, V. A.; Pozharskii, A. F.; Bienko, A. J.; Sawka-Dobrowolska, W. L.; Sobczyk, L. *J. Phys. Chem.* **2005**, *109*, 1637–1642.
(40) Tol, A. D.; Natu, A. D.; Puranik, V. G. *Mol. Cryst. Liq. Cryst.* **2007**, *469*, 69–77.
(41) Terao, H.; Gesing, T. M.; Ishihara, H.; Furukawa, Y.; Gowda, B. T. *Acta Crystallogr., Sect. E* **2008**, *65*, m323.
(42) Horn, C.; Scudder, M.; Dance, I. *Cryst. Eng. Comm.* **2000**, *9*, 53–66.
(43) Berkei, M.; Bickley, J. F.; Heaton, B. T.; Steiner, A. *Chem. Commun.* **2002**, 2180–2181.
(44) Chen, X.; Rickard, M. A.; Hull, J. W.; Zheng, C.; Leugers, A.; Simoncic, P. *Inorg. Chem.* **2010**, *49*, 8684–8689.
(45) Aragoni, M. C.; Arca, M.; Devillanova, F. A.; Hursthouse, M. B.; Huth, S. L.; Isaia, F.; Lippolis, V.; Mancini, A.; Verani, G. *Eur. J. Inorg. Chem.* **2008**, 3921–3928.
(46) Wang, Y. Q.; Wang, Z. M.; Liao, C. S.; Yan, C. H. *Acta Crystallogr., Sect. C* **1999**, *55*, 1503–1506.
(47) Shilov, G. V.; Kazheva, O. N.; Dyachenko, O. A.; Chernovyants, M. S.; Simonyan, S. S.; Goleva, V. E. *Russ. J. Phys. Chem.* **2002**, *76*, 1436–1443.
(48) Ogawa, Y.; Takahashi, O.; Kikuchi, O. *J. Mol. Struct.* **1998**, *429*, 187–196.
(49) Ghassemzadeh, M.; Dehnicke, K.; Goesmann, H.; Fenske, D. *Z. Naturforsch.* **1994**, *49b*, 602–608.
(50) Parigoridi, I. E.; Corban, G. J.; Hadjikakou, S. K.; Hadjiliadis, N.; Kourkoumelis, N.; Kostakis, G.; Psycharis, V.; Raptopoulouc, C. P.; Kubicki, M. *Dalton Trans.* **2008**, 5159–5165.
(51) Parlow, A.; Hartl, H. *Acta Crystallogr., Sect. B* **1979**, *35*, 1930–1933.
(52) Yagi, Y.; Popov, A. I. *J. Inorg. Nucl. Chem.* **1967**, *29*, 2223–2230.
(53) Bateman, R. J.; Bateman, L. R. *J. Am. Chem. Soc.* **1972**, *94*, 1130–1134.
(54) Asaji, T.; Eda, K.; Fujimori, H.; Adachi, T.; Shibusawa, T.; Oguni, M. *J. Mol. Struct.* **2007**, *826*, 24–28.